Supporting Information

Frick et al. 10.1073/pnas.1221489110

SI Materials and Methods

Beetle Rearing and Secretion Collection. *Phaedon cochleariae* (F.) was laboratory-reared as continuous cultures (York chamber, 15 °C and 16-h/8-h light/dark period) on leaves of *Brassica rapa* spp. Larval secretion was collected in glass capillaries (inner diameter = 0.28 mm, outer diameter = 0.78 mm, length = 100 mm; Hirschmann Laborgeraete, Eberstadt, Germany). Sealed capillaries containing samples were stored at −20 °C until needed. Secretions were weighed in the sealed capillaries on an ultramicrobalance (Mettler–Toledo) three times; the weight of empty capillaries was subtracted, and the final weight was averaged.

Isolation and Cloning of a cDNA encoding the *Phaedon cochleariae* isoprenyl diphosphate synthase 1 (*Pc*IDS1). Tissue samples from the head, gut, fat body, Malpighian tubules, and defensive glands were taken from third-instar larvae dissected in Ringer's solution (1) and directly transferred in liquid nitrogen-cooled reaction tubes. Total RNA was extracted with the RNeasy Micro Kit (Qiagen) according to the manufacturer's instructions. Complete removal of DNA was achieved using the RNase-free DNase Set (Qiagen). The quality of the RNA was evaluated by measuring the 260:280-nm absorbance ratio, and the integrity of 18S and 28S ribosomal RNA bands was assessed by electrophoresis on RNA 6000 Nano labchips (Agilent Technologies). RNA concentrations were determined from absorbance values at a wavelength of 260 nm. First-strand cDNA was subsequently transcribed from total RNA using SuperScript III reverse transcriptase (Life Technologies). Up to 1 μg of total RNA was reverse-transcribed according to the manufacturer's instructions using oligo$(dT)_{12–18}$ primer. Degenerated primers were designed against the highly conserved regions of previously identified short-chain isoprenyl diphosphate synthases (scIDSs) from *Myzus persicae*, *Aphis gossypii*, *Agrotis ipsilon*, and *Anthonomus grandis*. PCR amplification using Taq DNA Polymerase (Promega) of a 686-bp core fragment was performed with the primer pair FWD_211_geranyl diphosphate synthase (GDPS) (5′-TTC ATG G(AC)(ACT)(GT)(GT)(GC)TTCCC(AGC)GA-3′) and REV_903_GDPS (5′-GAAGTCAT(CT)(CT)TGA(AC)(CT)TTG-3′). The following cycling profile was carried out in an Eppendorf thermal cycler: 3 min at 94 °C; 35 cycles of 30 s at 94 °C, 30 s at 45 °C, and 1 min at 72 °C; and a final 10-min extension at 72 °C. PCR products were purified using QiaEx II (Qiagen), ligated into pCR2.1-TOPO vector (Life Technologies), and sequenced. To obtain full-length cDNA sequence of *P. cochleariae* isoprenyl diphosphate synthase (IDS), a BD SMART RACE cDNA Amplification Kit (BD Biosciences) was used. For amplification of the 5′-end, site sequence-specific reverse primers were designed as followed: RACE_5_214_Rev (5′-CCCTAGGATGCCGGCCAATCTCACG-3′) and nested primer RACE_5_140_Rev (5′-GTGGACAGGCCCCTGGTCTTCTTGC-3′). The sequence-specific primers for the 3′-end site were RACE_3_447_FWD (5′-GACCAACATGGGCCAATCTTTAGACGC-3′) and nested primer RACE_3_483_FWD (5′-GAAGGATGGGAGGCCCATATTGAGCC-3′). The 5′ and 3′ RACE products were cloned and sequenced. The resulting assembled cDNA sequence contained a 1,290-bp open-reading frame that encodes an IDS similar protein of 430 aa referred to here as *P. cochleariae* isoprenyl diphosphate synthase 1 (*Pc*IDS1). This sequence of *Pc*IDS1was registered at GenBank (accession no. KC109782).

Functional Expression and Purification of Recombinant *Pc*IDS1. The entire encoding sequence of *Pc*IDS1 lacking the predicted signal peptide (based on analysis with SignalP 4.1 (2), available at the prediction servers of the Center for Biological Sequence Analysis, Technical University of Denmark, Lyngby, Denmark) was amplified with the following primers that included the start and stop codons for translation in an *Escherichia coli*-based heterologous expression system: *Pc*IDS1-forward (5′-CACCAGGGCCCTCTCCACGATC-3′) and *Pc*IDS1-reverse (5′-CTATGCATCCCTCTTGTAAATCTTCTT-3′). Template cDNA was synthesized by RT from RNA of whole-body *P. cochleariae* larvae, except for the gut tissue. PCR was performed using an Expand High Fidelity PCR system (Roche Applied Science). PCR was performed for 3 min at 94 °C for denaturation, followed by 10 cycles of 15 s at 94 °C, 30 s at 55 °C, and 90 s at 72 °C; 20 cycles of 15 s at 94 °C, 30 s at 55 °C, and 90 s plus 5 s of elongation for each cycle at 72 °C; and a final extension for 7 min at 72 °C. The resulting cDNA fragment was purified with the Zymoclean Gel DNA Recovery Kit (Zymo) and cloned in the expression vector pET100/D-TOPO (Invitrogen), which has a 6 × His-tag on the N terminus. Plasmids were transferred into the strain *E. coli* TOP10F (Life Technologies) and sequenced. Positive constructs were then transferred into different expression strains, including BL21(DE3) star (Invitrogen), BL21(DE3) pLysS (Life Technologies), and Rosetta (DE3; Novagen), but strain BL21(DE3) star produced the highest amount of soluble and active protein of long and short *Pc*IDS1. Bacterial precultures of 20 mL were grown over 3 d at 18 °C under continuous rotation on LB with 50 μg/mL carbenicillin. Afterward, the cells were pelleted and used to inoculate the 200-mL expression culture. There, we used the Overnight Express Autoinduction System 1 (Novagen) and let them grow over 2 d at 18 °C under continuous rotation to stationary phase according to the manufacturer's recommendations. Bacterial pellets were resuspended in 2 mL of assay buffer containing 25 mM 3-(*N*-morpholino)-2-hydroxypropanesulfonic acid (MOPSO; pH 7.3), 10% (vol/vol) glycerol, and 150 mM NaCl. The suspension was sonicated using a Sonopuls HD2070 (Bandelin) for 4 min, cycle 2, at 60% power. The overexpressed His-tagged proteins were subsequently column-purified by affinity chromatography with Ni-nitrilotriacetic acid agarose columns (Qiagen) using a stepwise imidazole gradient from 10 to 500 mM. The purity of the recombinant proteins was evaluated by SDS/PAGE gel electrophoresis, followed by colloidal Coomassie staining (Roti-Blue Colloidal Coomassie Staining; Carl Roth). The purified *Pc*IDS1 migrated at ∼45.8 kDa (399 aa). Fractions that contained the highest amount of pure recombinant protein were pooled and desalted in assay buffer with a PD-10 Desalting column (Amersham Biosciences) to remove the imidazole.

To see if the affinity tag influenced the enzyme activity, the fusion protein *Pc*IDS1 was subsequently cleaved using the highly specific serine protease EnterokinaseMax (Life Technologies) according to the manufacturer's instructions. After purification and removal of the affinity tag, cleavage was checked by SDS/PAGE and Western blotting using the anti-His antibody. The fusion protein and the cleaved protein were tested for their enzyme activity. Because cleavage of the tag altered neither the activity nor the product profile, the truncated His-tagged fusion protein *Pc*IDS1 was used in all following experiments.

To determine the conformational state of the *Pc*IDS1 quaternary structure, size exclusion chromatography was performed. The protein was added to running buffer [25 mM MOPSO (pH 7.3), 10% (vol/vol) glycerol, and 150 mM NaCl] in the presence of either 5 mM $MgCl_2$ or 0.5 mM $CoCl_2$ and incubated for 10

min at 4 °C. To confirm the overall conformation of the protein with the different metal cofactors, an aliquot of each solution was separated on a SuperdexHiLoad 16/60 200 prep grade (GE Healthcare) column at a flow rate of 1 mL/min. The retention volume of *Pc*IDS1 was detected via its absorption at 280 nm. To calibrated the column, we used cytochrome *c* from horse heart (12.4 kDa), carbonic anhydrase from bovine erythrocytes (29 kDa), BSA (66 kDa), alcohol dehydrogenase from yeast (150 kDa), and β-amylase from sweet potato (200 kDa) in the presence of 10 mM $CoCl_2$ or 10 mM $MgCl_2$. The molecular weight for *Pc*IDS1 was calculated by the formula received from the corresponding standard curve. Without cofactor, $y = -27.133x + 128.38$ ($R^2 = 0.9925$); with Co^{2+}, $y = -27.133x + 128.21$ ($R^2 = 0.9927$); and with Mg^{2+}, $y = -27.122x + 128.26$ ($R^2 = 0.9921$).

Prenyltransferase Assay and Product Distribution Analyses. For kinetic analyses, enzyme assays of *Pc*IDS1 were carried out in a final volume of 200 μL containing 25 mM MOPSO (pH 7.3), 10% (vol/vol) glycerol, 150 mM NaCl, and 5 mM Mg^{2+} or 1 mM Co^{2+}, respectively. As substrates and countersubstrates, isopentenyl diphosphate (IDP), dimethylallyl diphosphate, and geranyl diphosphate (GDP; Sigma–Aldrich) were used. The countersubstrate concentration was kept constant at 50 μM; different experimental conditions are mentioned separately. The analyzed substrate ranged from 0.1 μM up to 100 μM. The reaction was heated to 30 °C and initiated by adding 0.2 μg of protein for Co^{2+} assays or 2 μg of protein for Mg^{2+} assays of the recombinant protein, and it was then incubated further at 30 °C. The water phase was analyzed by direct injection of 1 μL into the HPLC system at different time points from the same reaction mixture to identify the linear reaction velocity for every parameter. Calculation of the kinetic parameters was performed with GraphPad Prism version 5.04 (GraphPad Software) using the built-in enzyme kinetics module.

The pH optimum for the catalytic activity of *Pc*IDS1 was determined to be 7.0–7.5 in the presence of Mg^{2+} or Co^{2+}. However, the enzyme activity was quite stable over a broad range, from pH 4 to pH 8. Even the temperature optimum was not delimited to a narrow range. Acceptable activity with Mg^{2+} or Co^{2+} was measured from 15 °C up to 45 °C, whereas the optimum resided at 28 °C to 32 °C.

Activity testing of purified full-length *Pc*IDS1 in the presence of Mg^{2+} or Co^{2+} showed only about 5% of the activity in both cases in comparison to its truncated form, which lacks the predicted signal sequence.

For enzyme assay from larvae material, the samples were obtained by macerating different tissues with a 2-mL Potter–Elvehjem grinder with a Teflon pestle for 2 min at 4 °C with 300 μL of assay buffer. The suspension was centrifuged at 20,000 × *g*, and the protein concentration of the supernatant was determined. Ten micrograms of protein was used for standard assays and incubated at 30 °C for 60 min. The assays were stopped by adding 500 μL of chloroform and by mixing for 20 s, followed by centrifugation for 5 min at 5,000 × *g*. Subsequently, the water phase was transferred to a glass vial and measured directly by injecting 1 μL into the HPLC system. Protein concentrations were measured according to Bradford and Williams (3) and Bradford (4), using the Coomassie Plus Protein Assay Kit (Thermo Scientific Pierce) with BSA as a standard.

Liquid Chromatography-Tandem MS Method for *Pc*IDS1 Assay Product Determination. Analysis of isoprenoid diphosphates (IDS) was performed according to a modified method (5) on an Agilent 1260 HPLC system (Agilent Technologies) coupled to an API 5000 triple-quadrupole mass spectrometer (AB Sciex Instruments). For separation, a ZORBAX Extended C-18 column (1.8 μm, 50 mm × 4.6 mm; Agilent Technologies) was used. The mobile phase consisted of 5 mM ammonium bicarbonate in water as solvent A and acetonitrile as solvent B, with the flow rate set at 1.2 mL/min and the column temperature kept at 20 °C. Separation was achieved by using a gradient starting at 0% B, increasing to 90% B in 3 min and 100% B in 3.1 min (1-min hold), followed by a change to 0% B in 0.5 min (2.5-min hold) before the next injection. The injection volume for samples and standards [GDP and farnesyl diphosphate (FDP) from Sigma–Aldrich] was 1 μL; autosampler temperature was either 30 °C for assays without or 4 °C for assays with chloroform extraction. The mass spectrometer was used in the negative electrospray ionization (EI) mode. Optimal settings were determined using standards. Levels of ion source gases 1 and 2 were set at 60 and 70 psi, respectively, with a temperature of 700 °C. Curtain gas was set at 30 psi and collision gas was set at 7 psi, with all gases being nitrogen. Ion spray voltage was maintained at −4,200 V. Multiple-reaction monitoring (MRM) was used to monitor analyte parent ion-to-product ion formation: *m*/*z* 312.9/79 for GDP and *m*/*z* 380.9/79 for (*E*,*E*)-FDP. *Cisoid* products like neryl-diphosphate, (*Z*,*E*)-FDP, or (*Z*,*Z*)-FDP were not detected. Detection of GDP was omitted when used as substrate. Data analysis was performed using Analyst Software 1.6 Build 3773 (AB Sciex).

***Pc*IDS1 Antibody Production and Immunoblot Analysis.** For synthesis of polyclonal antibodies, a 16-aa peptide (HDLFFKIMKKIYKRDA) from the N-terminal end of the protein was used. The antibody was affinity-purified with 3 mg epoxy-immobilized antigen that was used for immunization (Davids Biotechnologie).

For immunoblot analysis, crude protein from different larval tissue was extracted in assay buffer as described above. Equal amounts of 5 μg of total protein of each tissue were separated by SDS/PAGE using any-KD acrylamide gels (BIO-RAD). Afterward, the proteins were transferred electrophoretically onto nitrocellulose membranes (BIO-RAD). Membranes were blocked with TBST [20 mM Tris (pH 7.5), 150 mM NaCl, 0.1% (vol/vol) Tween 20] and 10% nonfat milk, followed by incubation with 1:100 of the polyclonal anti-*Pc*IDS1 antibody at 16 °C overnight. After washing with blocking solution and a subsequent incubation with anti-rabbit HRP-conjugated secondary antibody, a final TBST washing was carried out. Signal detection was achieved by enhanced chemiluminescence (Thermo Scientific) and Amersham Hyperfilm ECL (GE Healthcare).

Sequence Comparison and Homology Modeling. Sequence similarity searches were performed using the alignment tool BLAST (6). Nucleotide sequences of different organisms were downloaded from the National Center for Biotechnology Information. To determine the degree of similarity between the members of insect scIDS and full-length *Pc*IDS1, sequence analysis was performed using the ClustalW tool (Lasergene 10 Core Suite; DNASTAR).

The 3D structure of truncated *Pc*IDS1 was modeled using the molecular modeling software YASARA (7). YASARA identified 15 templates based on alignment scores and low E-values suitable for homology modeling. Altogether, 32 models were automatically created and subsequently refined. The model based on the X-ray structure of FDP synthase from *Homo sapiens* deposited in the protein database (1zw5; see www.rcsb.org) (8, 9) appeared to be the most useful one. The structure of the model of *Pc*IDS1 has been deposited at the Protein Model DataBase (http://mi.caspur.it/PMDB/main.php) (10) and has been assigned the ID code PM0078683 for free download. The Mg^{2+} and the ligand binding position of IDP were automatically imported from the template's X-ray structure. The artificial cocrystallized zoledronic acid, [1-hydroxy-2-(1H-imidazol-1-yl)ethane-1,1-diyl]bis(phosphonic acid), was manually replaced by GDP. This model was then refined with the md-refinement tool of YASARA (7). The quality of the final model was checked with PROSA II (11) and PROCHECK (12). The graphical analysis with PROSA II showed one small loop (10 aa) area in positive energy range out-

side the active site. A combined energy z-score of −9.83 clearly indicated a native-like folded structure. Analysis of the calculated model with PROCHECK evaluated the consistency of all stereochemical parameters, such as the Ramachandran plot quality (92.3% of the backbone dihedral angles in most favored areas).

To investigate influences by the replacement of Mg^{2+} with Co^{2+}, the TRIPOS force field was used first (13). Thus, the atom types of Mg^{2+} were modified to Co^{2+}, and short molecular dynamics simulations (10 ps, 300 K) with subsequent energy minimization of GDP in the active site were performed. The Co^{2+} and the interacting side chains of all remaining amino acids except this ligand were kept fixed because the TRIPOS force field is not suitable for protein structure refinement. To estimate the interaction energies of different ions with the diphosphate moiety and aspartate side chains, density functional theory (DFT) B3LYP 6-311G++ calculations were performed using Gaussian 03 (14).

Tissue-Specific Expression of *Pc*IDS1. Quantitative real-time PCR was used for relative quantification (15). cDNA was synthesized from DNA-digested RNA and purified from three larvae per biological replicate using the RNAqueous Micro Kit (Life Technologies). Three biological replicates were analyzed twice. If technical replicates had a difference in the quantification cycle value greater than 1, the assay was repeated. Reference genes [*Pc*RPL8 (EMBL: AFQ22729.1) and *Pc*RPS3 (GenBank: KC109783)] were chosen. Real-time PCR data were acquired on an Mx3000P Real-Time PCR system (Agilent) using Brilliant III SYBR Green qPCR Master Mix (Agilent) according to the manufacturer's instructions. These analyses were performed following the minimum information for publication of quantitative real-time PCR experiments guidelines (16, 17).

RNAi in *P. cochleariae* Larvae. dsRNA was synthesized using the Megascript RNAi kit (Life Technologies) with altering of the elution buffer to 3.5 mM Tris·HCl, 1 mM NaCl, 50 nM Na_2HPO_4, 20 nM KH_2PO_4, 3 mM KCl, and 0.3 mM EDTA (pH 7.0). Off-target prediction was performed for highly specific silencing according to Bodemann et al. (18). The ORFs of full-length *PcIDS1* and *Gfp* were analyzed for off-target prediction by dicing the sequences *in silico* (19) and using the resulting putative 21-nt siRNAs for a BLASTn search linked to our transcriptome database of *P. cochleariae*. No putative off-target effects with other transcripts are predicted with the chosen dsRNA sequences on a critical value of at least 20 continuous nucleotides that have to be identical. The dsRNA synthesis templates with opposite T7-promotor sites were amplified out of sequenced plasmid pIB/V5-His (Life Technologies) containing full-length *PcIDS1* for 850 bp of *PcIDS1* using IDS1_FWD_T7_RNA (5′-TAATACGACTCACTATAGGGAGATCAAGCCAGTCTCCT-3′) as forward primer and IDS1_REV_T7_RNA (5′-TAATACGACTCACTATAGGGAGACTAAGCATCCCTCTTG-3′) as reverse primer and pCR3.1/CT-GFP-TOPO (Life Technologies) for 720 bp of *Gfp* (for primer, see ref. 18), respectively. The concentration of dsRNA was adjusted to 2 μg/μL, and for all injections, 250 nL (500 ng) of dsRNA solution was used.

Late first-instar larvae of *P. cochleariae* were used for injections. These were collected 5 d after hatching and were put in an incubator set to 16 h of light at 14 °C and 8 h of darkness at 12 °C for slow larval development after treatment. A Nano2000 injector (WPI) on a three-axis micromanipulator was used for injecting ice-chilled larvae parasagittal between the pro- and mesothorax.

Relative Quantification of 8-Hydroxygeraniol-Glucoside in *P. cochleariae* Fat Body and Hemolymph. Analysis was done on an Agilent 1260 HPLC system (Agilent Technologies) coupled to an API 5000 triple-quadrupole mass spectrometer (AB Sciex Instruments). For separation, a ZORBAX Eclipse XDB-C-18 column (1.8 μm, 50 mm × 4.6 mm; Agilent Technologies) was used. The mobile phase consisted of 20 mM ammonium formate in water as solvent A and acetonitrile as solvent B, with the flow rate set at 1.0 mL/min and the column temperature kept at 20 °C. Separation was achieved by using a gradient starting at 10% solvent B, increasing to 95% solvent B in 5 min (1-min hold), followed by a change to 10% solvent B in 1 min (1-min hold) before the next injection. Injection volume for samples and standards was 5 μL; the autosampler temperature was 4 °C. The mass spectrometer was used in negative EI mode. Optimal settings were determined using a standard. Ion source gases 1 and 2 were set at 70 psi, with a temperature of 700 °C. Curtain gas was set at 25 psi and collision gas was set at 6 psi, with all gases being nitrogen. Ion spray voltage was maintained at −3000 V. The monitored MRM transition was *m/z* 377.3/331.2. Data analysis was performed using Analyst Software 1.6 Build 3773 (AB Sciex).

Relative Quantification of Chrysomelidial in Defense Secretions of *P. cochleariae*. Secretions were collected and weighed in pulled-out glass capillaries from different instar stages of treated larvae, and they were then diluted 1:200 (wt/vol) in ethyl acetate supplemented with 100 μg/mL methyl benzoate as an internal standard. One microliter was subjected to GC-EI-MS analysis [ThermoQuest Finnigan ITQ GC-MS 2000 (quadrupole) equipped with Phenomenex ZB-5-W/Guardian-column, 25 m (10-m Guardian precolumn) × 0.25 mm, film thickness of 0.25 μm]. Substances were separated splitless using helium as a carrier (1.5 mL/min). Conditions were set as follows: 50 °C (2 min), 20 °C/min to 130 °C, 40 °C/min to 200 °C, 20 °C/min to 220 °C, and 40 °C/min to 300 °C (1 min). Inlet temperature was 220 °C, and transfer line temperature was 280 °C. Chrysomelidial was identified according to Oldham et al. (20). The peak areas were obtained using the Interactive Chemical Information System algorithm that is implemented in the Xcalibur bundle (version 2.0.7; Thermo Scientific). The relative amount of chrysomelidial per larva has been calculated with the following equation, in which *mChry* is the relative amount of chrysomelidial per larva, *AoChry* is the peak area of chrysomelidial, *AoMB* is the peak area of methyl benzoate, and *mSec* is the average mass of secretion per larva:

$$mChry = \left(\frac{AoChry}{AoMB} * dilution\right) * mSec.$$

Fitness Measurements. The development of larval weight was documented using five replicates of three larvae. Larval weight was measured per replicate on an ultramicrobalance in a 24-h ± 3-h period. In accordance with the method used by Kuehnle and Mueller (21), the relative growth rate was calculated using the weight of freshly emerged pupae as the final larval developmental stage.

1. Discher S, et al. (2009) A versatile transport network for sequestering and excreting plant glycosides in leaf beetles provides an evolutionary flexible defense strategy. *ChemBioChem* 10(13):2223–2229.
2. Petersen TN, Brunak S, von Heijne G, Nielsen H (2011) SignalP 4.0: Discriminating signal peptides from transmembrane regions. *Nat Methods* 8(10):785–786.
3. Bradford MM, Williams WL (1976) New, rapid, sensitive method for protein determination. *Fed Proc* 35(3):274.
4. Bradford MM (1976) A rapid and sensitive method for the quantitation of microgram quantities of protein utilizing the principle of protein-dye binding. *Anal Biochem* 72(1-2):248–254.
5. Nagel R, Gershenzon J, Schmidt A (2012) Nonradioactive assay for detecting isoprenyl diphosphate synthase activity in crude plant extracts using liquid chromatography coupled with tandem mass spectrometry. *Anal Biochem* 422(1):33–38.

6. Altschul SF, Lipman DJ (1990) Protein database searches for multiple alignments. *Proc Natl Acad Sci USA* 87(14):5509–5513.
7. Krieger E, et al. (2009) Improving physical realism, stereochemistry, and side-chain accuracy in homology modeling: Four approaches that performed well in CASP8. *Proteins* 77(Suppl 9):114–122.
8. Kavanagh KL, Dunford JE, Bunkoczi G, Russell RG, Oppermann U (2006) The crystal structure of human geranylgeranyl pyrophosphate synthase reveals a novel hexameric arrangement and inhibitory product binding. *J Biol Chem* 281(31):22004–22012.
9. Kavanagh KL, et al. (2006) The molecular mechanism of nitrogen-containing bisphosphonates as antiosteoporosis drugs. *Proc Natl Acad Sci USA* 103(20): 7829–7834.
10. Castrignanò T, De Meo PD, Cozzetto D, Talamo IG, Tramontano A (2006) The PMDB Protein Model Database. *Nucleic Acids Res* 34:D306–D309.
11. Sippl MJ (1990) Calculation of conformational ensembles from potentials of mean force. An approach to the knowledge-based prediction of local structures in globular proteins. *J Mol Biol* 213(4):859–883.
12. Laskowski RA, MacArthur MW, Moss DS, Thornton JM (1993) PROCHECK—A program to check the stereochemical quality of protein structures. *J Appl Cryst* 26(2):283–291.
13. Clark M, Cramer RD, Van Opdenbosch N (1989) Validation of the General Purpose Tripos 5.2 Force Field. *J Comp Chem* 10(8):982–1012.
14. Frisch MJ, et al. (2004) Gaussian 03, Revision C.02. (Gaussian, Wallingford CT).
15. Livak KJ, Schmittgen TD (2001) Analysis of relative gene expression data using real-time quantitative PCR and the $2^{(-\Delta\Delta C(T))}$ Method. *Methods* 25(4):402–408.
16. Bustin SA, et al. (2010) MIQE précis: Practical implementation of minimum standard guidelines for fluorescence-based quantitative real-time PCR experiments. *BMC Mol Biol* 11:74–78.
17. Bustin SA, Johnson G, Agrawal SG (2012) [MIQE—Guidelines for developing robust real-time PCR assays]. *Mycoses* 55(Suppl 2):30–34. German.
18. Bodemann RR, et al. (2012) Precise RNAi-mediated silencing of metabolically active proteins in the defence secretions of juvenile leaf beetles. *Proc Biol Sci* 279(1745):4126–4134.
19. Naito Y, et al. (2005) dsCheck: Highly sensitive off-target search software for double-stranded RNA-mediated RNA interference. *Nucleic Acids Res* 33(Web Server issue): W589-91.
20. Oldham NJ, Veith M, Boland W, Dettner K (1996) Iridoid monoterpene biosynthesis in insects—Evidence for a *de novo* pathway occurring in the defensive glands of *Phaedon armoraciae* (Chrysomelidae) leaf beetle larvae. *Naturwissenschaften* 83(10): 470–473.
21. Kuehnle A, Mueller C (2011) Responses of an oligophagous beetle species to rearing for several generations on alternative host-plant species. *Ecol Entomol* 36(2):125–134.

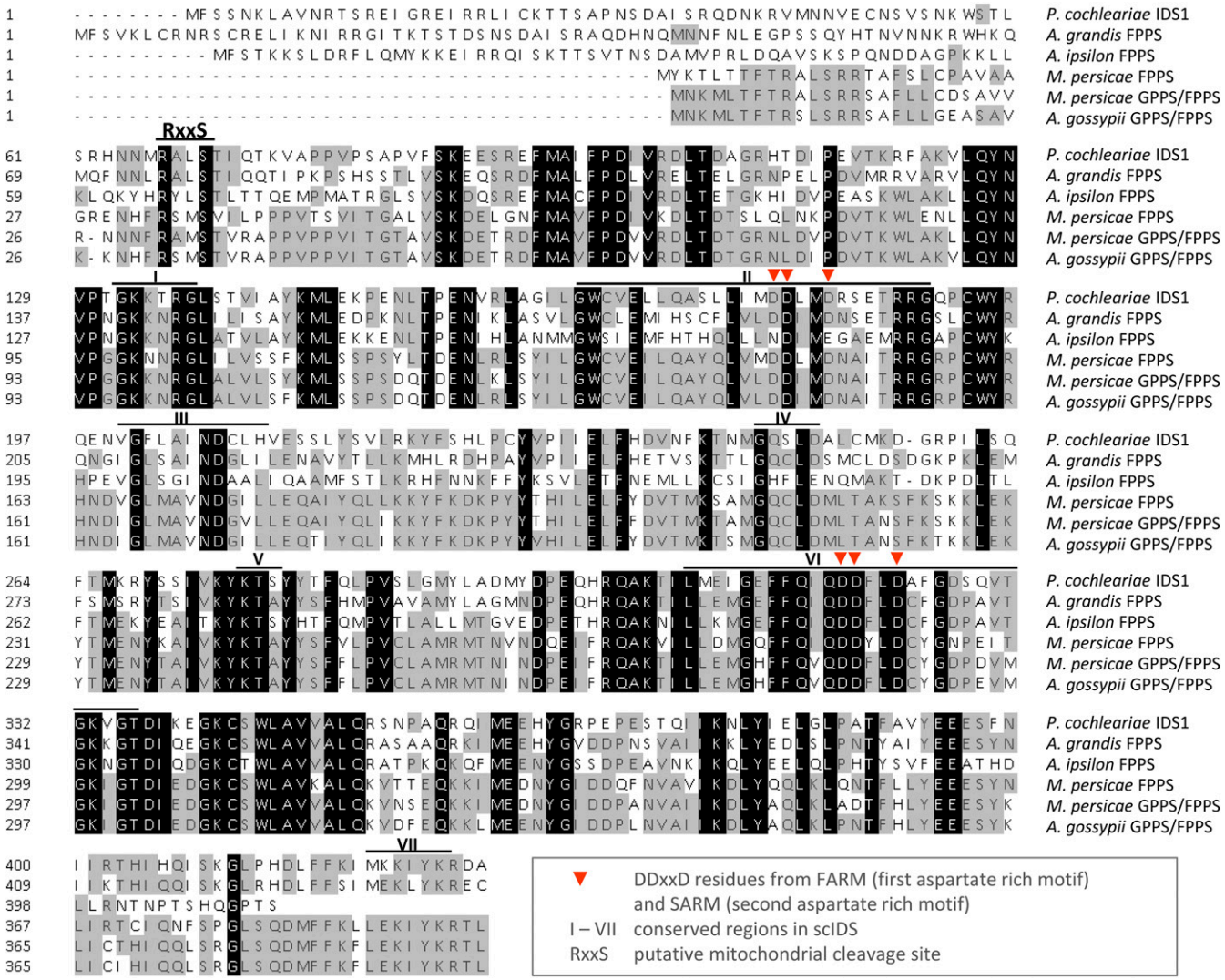

Fig. S1. Amino acid alignment (ClustalW) of full-length *Pc*IDS1 from *P. cochleariae* with other insect scIDSs. Sequence identity to other farnesyl diphosphate synthases (FDPSs): *Anthonomus grandis* (54.1%) (GenBank: AAX78434), *Myzus persicae* (45.4%) (GenBank: ABY19313), and *Agrotis ipsilon* (45.2%) (GenBank CAA08918). Sequence identity to bifunctional FDPSs/GDPSs: *Aphis gossypii* (48.6%) (EMBL: ACT79808) and *M. persicae* (48.4%) (EMBL: ABY19312). (Residues in black are identical in all sequences; gray residues are >50% identical in aligned sequences.)

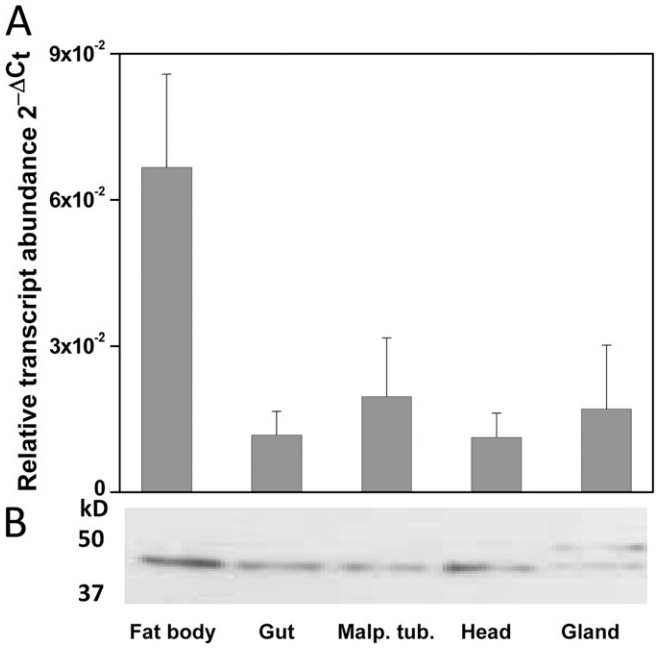

Fig. S2. (*A*) Relative transcript abundance ($2^{\Delta Ct}$) of *PcIDS1* in different larval tissues. (*B*) Western blot analyses of 5 μg of protein per lane probed with sequence-specific antibodies against *Pc*IDS1, followed by ECL detection. Malp. tub, Malpighian tubules.

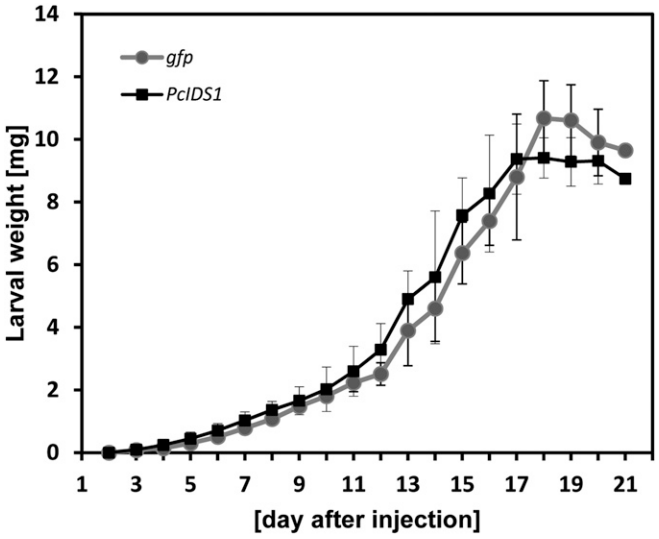

Fig. S3. Relative growth rate of RNAi-induced larvae from *P. cochleariae*. The development of larval weight was documented and measured in a 24-h ± 3-h period. No significant differences in the relative growth rate were observed between *Gfp*- and *PcIDS1*-injected larvae. The final larval developmental stage was the weight of freshly emerged pupae (n = 15, ±SD).

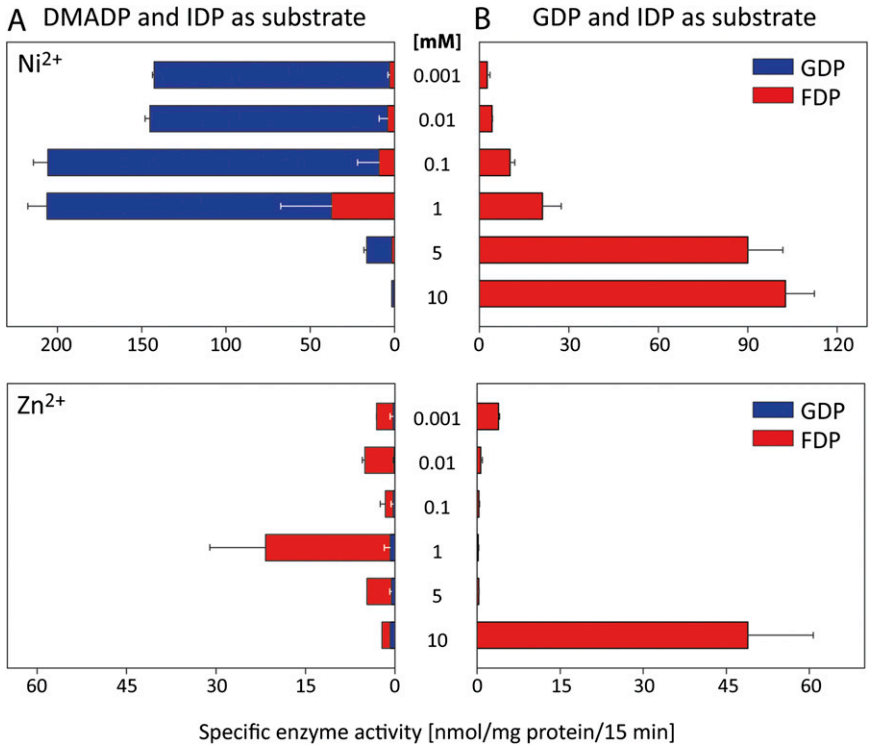

Fig. S4. Effect of metal cofactors regarding product formation and enzyme activity of *Pc*IDS1. (*A*) Different concentrations of Ni^{2+} and Zn^{2+} were added to *Pc*IDS1 and incubated with 50 μM IDP and 50 μM dimethylallyl diphosphate (DMADP; $n = 3$, ±SD). (*B*) Different concentrations of Ni^{2+} and Zn^{2+} were added to *Pc*IDS1 and incubated with 50 μM IDP and 50 μM GDP ($n = 3$, ±SD).

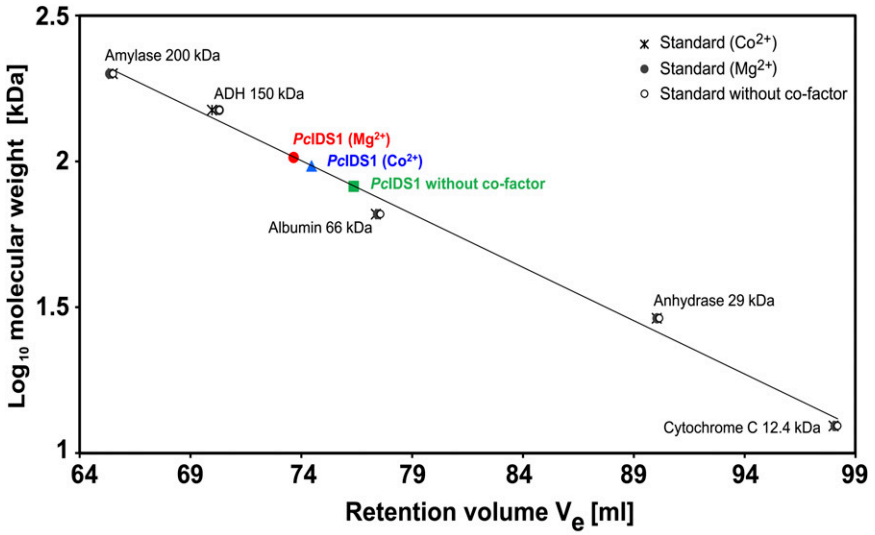

	Elution volume			MW log10			calc. MW (kDa)		
	No co-factor	Co^{2+}	Mg^{2+}	No co-factor	Co^{2+}	Mg^{2+}	No co-factor	Co^{2+}	Mg^{2+}
*Pc*IDS1	76.3	74.4	73.6	1.91	1.98	2.01	74.6	87.6	93.8
Amylase	65.5	65.4	65.3	2.31	2.31	2.31	207.5	204.9	208.5
ADH	70.3	69.9	70.2	2.14	2.14	2.13	138.1	140.1	137.2
Albumin	77.5	77.3	77.4	1.87	1.87	1.87	74.5	74.8	74.7
Anhydrase	90.1	90.0	90.0	1.40	1.40	1.40	25.6	25.5	25.6
Cytochrome C	98.1	98.0	98.0	1.11	1.11	1.11	12.9	12.9	12.9

Fig. S5. Analytical size exclusion chromatography of *Pc*IDS1. The plot shows the relative retention volumes of the protein molecular weight standards and the calculated standard curve by linear regression dependent on the divalent ions. The relative retention volumes of the apoprotein *Pc*IDS1 are shown by the green rectangle. The shifts of the retention volume dependent on the divalent metal cofactor are represented by the red dot in the presence of Mg^{2+} and the blue triangle in the presence of Co^{2+}.

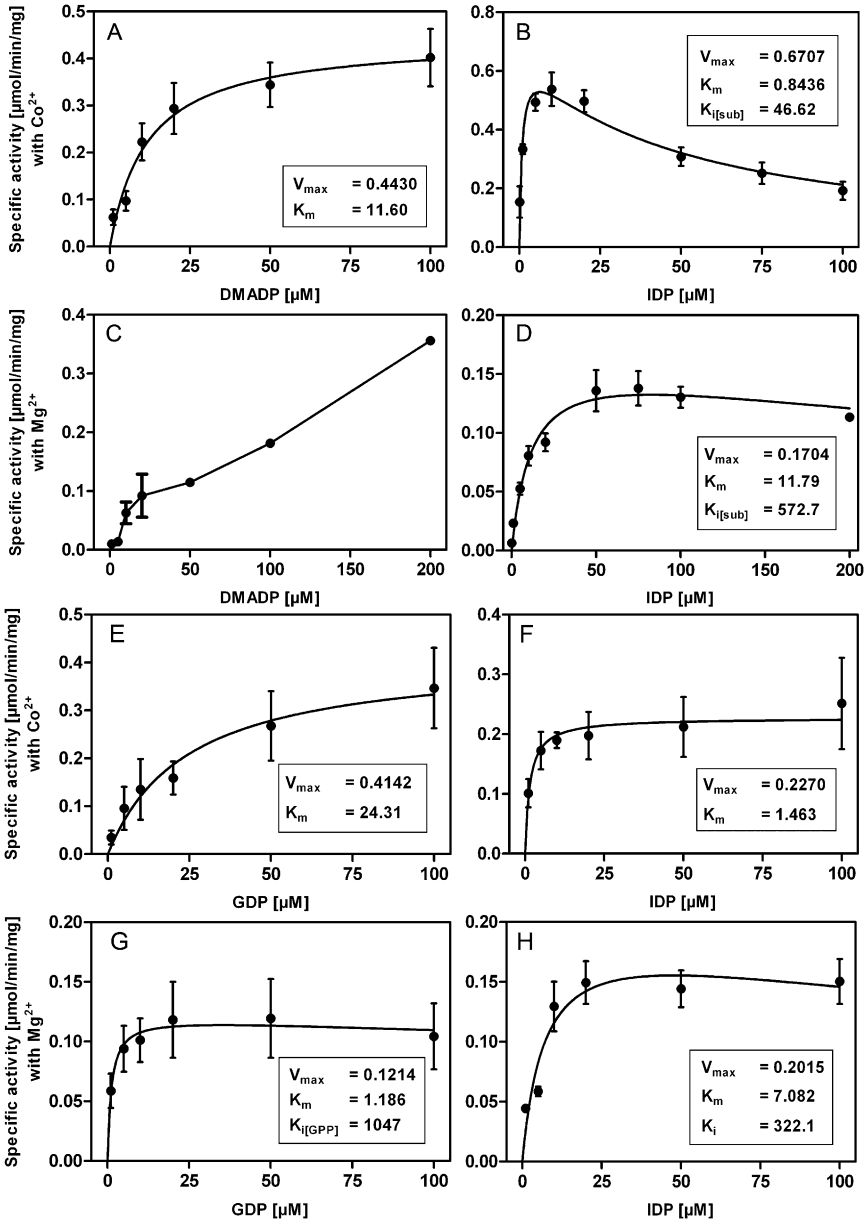

Fig. S6. Kinetic analyses of *Pc*IDS1 with nonlinear regression and built-in function calculated with GraphPad Prism version 5.04. (*A*) Calculation according to the Michaelis–Menten kinetic of $K_{m(DMADP)}$ with Co^{2+} and 15 µM IDP. (*B*) Calculation with substrate inhibition of $K_{m(IDP)}$ with Co^{2+} and 50 µM dimethylallyl diphosphate (DMADP). (*C*) Enzyme activity data with variable DMADP in the presence of Mg^{2+} and 50 µM IDP. (*D*) Calculation with substrate inhibition of $K_{m(IDP)}$with Mg^{2+} and 50 µM DMADP. (*E*) Calculation according to the Michaelis–Menten kinetic of $K_{m(GDP)}$ with Co^{2+} and 50 µM IDP as countersubstrate. (*F*) Calculation according to the Michaelis–Menten kinetic of $K_{m(IDP)}$ with Co^{2+} and 50 µM GDP as countersubstrate. (*G*) Calculation with substrate inhibition of $K_{m(GDP)}$ with Mg^{2+} and 50 µM IDP as countersubstrate. (*H*) Calculation with substrate inhibition of $K_{m(IDP)}$ with Mg^{2+} and 50 µM GDP as countersubstrate.

Table S1. Enzyme activity of *Pc*IDS1 with different metal cofactors

Substrate	Ion	Optimal cofactor concentration, mM	Total activity, nmol/mg of protein per 15 min (±SD)	GDP activity, % of total activity
DMADP	Co^{2+}	0.5	1,022.33 (±72.2)	95.9
	Mg^{2+}	5	418.85 (±6.2)	18.3
	Mn^{2+}	0.5	239.66 (±16.2)	98.8
	Ni^{2+}	0.1	206.8 (±41.3)	81.9
	Zn^{2+}	0.1	21.69 (±24.1)	96.3
GDP	Co^{2+}	0.01	333.56 (±48.13)	
	Mg^{2+}	0.5	967.25 (±136.4)	
	Mn^{2+}	0.01	785.07 (±136.5)	
	Ni^{2+}	0.001	102.68 (±9.6)	
	Zn^{2+}	0.001	48.90 (±11.8)	

DMADP, dimethylallyl diphosphate.

Table S2. ICP-OES and ICP-MS analyses of fat body and gut tissue of *P. cochleariae* larvae

		Fat body 1		Fat body 2		Gut	
Element	Method	DW, μg/g (±SD)	DW, μmol/g	DW, μg/g (±SD)	DW, μmol/g	DW, μg/g (±SD)	DW, μmol/g
Ca	ICP-OES	753.2 (±0.3)	18.7	788 (±16)	19.6	893 (±12)	22.2
Co	ICP-MS	0.243 (±0.005)	0.0041	0.198 (±0.005)	0.0033	0.297 (±0.001)	0.005
Cu	ICP-MS	14.09 (±0.07)	0.221	14.9 (±0.2)	0.234	12.88 (±0.03)	0.203
Fe	ICP-MS	41.7 (±0.1)	0.746	41.8 (±0.5)	0.748	92.6 (±0.04)	1.658
K	ICP-OES	12,075 (±274)	308.8	12,112 (±71)	309.8	18,299 (±4)	468
Mg	ICP-OES	2,223 (±41)	91.4	2,255.5 (±0.5)	92.8	2,205.2 (±0.4)	90.7
Mn	ICP-MS	16.51 (±0.04)	0.301	16.706 (±0.002)	0.304	47.3 (±0.4)	0.861
Na	ICP-OES	462 (±11)	20.1	463 (±5)	20.1	499.2 (±0.4)	21.7
Ni	ICP-MS	0.36 (±0.01)	0.0061	0.3598 (±0.0007)	0.0061	0.88 (±0.08)	0.0149
Zn	ICP-MS	62.3 (±0.3)	0.952	62.66 (±0.02)	0.958	141.1 (±0.03)	2.158

DW, dry weight; ICP-MS, inductively coupled plasma mass spectrometry; ICP-OES, inductively coupled plasma optical emission spectrometry.

Table S3. Energies of the compounds and resulting reaction energies for the formation of diphosphate metal complexes in kilocalories per mole calculated with density functional theory (DFT) B3LYP 6-311G++ (d.p)

	Products energy	Educts energy			
X	X-DP^{3-}	X	DP^{3-}	Reaction energy	Δ to Mg^{2+}
Mg^{2+}	−885,175.2	−125,023.7	−759,218.5	−933.0	0
Co^{2+}	−16,277,257.6	−867,059.6	−759,218.5	−979.6	−46.6
Mn^{2+}	−1,481,820.2	−721,619.3	−759,218.5	−982.4	−49.4

X, metal cation.

Table S4. Energies of the compounds and resulting reaction energies for the formation of propionic acid metal complexes in kilocalories per mole calculated with DFT B3LYP 6-311G++ (d.p)

	Products energy	Educts energy			
X	$X(CH_3CH_2COO^-)_2$	X	$(CH_3CH_2COO^-)_2$	Reaction energy	Δ to Mg^{2+}
Mg^{2+}	−461,861.2	−125,023.7	−336,166.4	−671.1	0
Co^{2+}	−1,203,933.8	−867,059.6	−336,166.4	−712.6	−41.5
Mn^{2+}	−1,058,498.3	−721,619.3	−336,166.4	−707.8	−36.7

X, metal cation.

Table S5. Energies of the compounds and resulting reaction energies for the formation of metal complexes with both propionic acid and diphosphate using the metal cation diphosphate complex as educt in kilocalories per mole calculated with DFT B3LYP 6-311G++ (d.p)

	Products energy	Educts energy			
X	$CH_3CH_2COO^- \times (P_2O_7H_3)^-$	X $(P_2O_7H_3)^-$	$CH_3CH_2COO^-$	Reaction energy	Δ to Mg^{2+}
Mg^{2+}	−1,054,033.6	−885,711.5	−168,083.2	−238.9	0
Co^{2+}	−1,796,098.5	−1,627,782.5	−168,083.2	−232.8	6.1
Mn^{2+}	−1,650,660.9	−1,482,341.6	−168,083.2	−236.1	2.8

X, metal cation.

Table S6. Energies of the compounds and resulting reaction energies for the formation of metal complexes with both propionic acid and diphosphate using the metal cation propionic acid complex as educt in kilocalories per mole calculated with DFT B3LYP 6-311G++ (d.p)

	Products energy	Educts energy			
X	$CH_3CH_2COO^- \times (P_2O_7H_3)^-$	$(P_2O_7H_3)^-$	$CH_3CH_2COO^-$ X	Reaction energy	Δ to Mg^{2+}
Mg^{2+}	−1,054,033.6	−760,331.1	−293,532.0	−170.5	0
Co^{2+}	−1,796,098.5	−760,331.1	−1,035,599.4	−168.0	2.5
Mn^{2+}	−1,650,660.9	−760,331.1	−890,171.2	−158.6	11.9

X, metal cation.